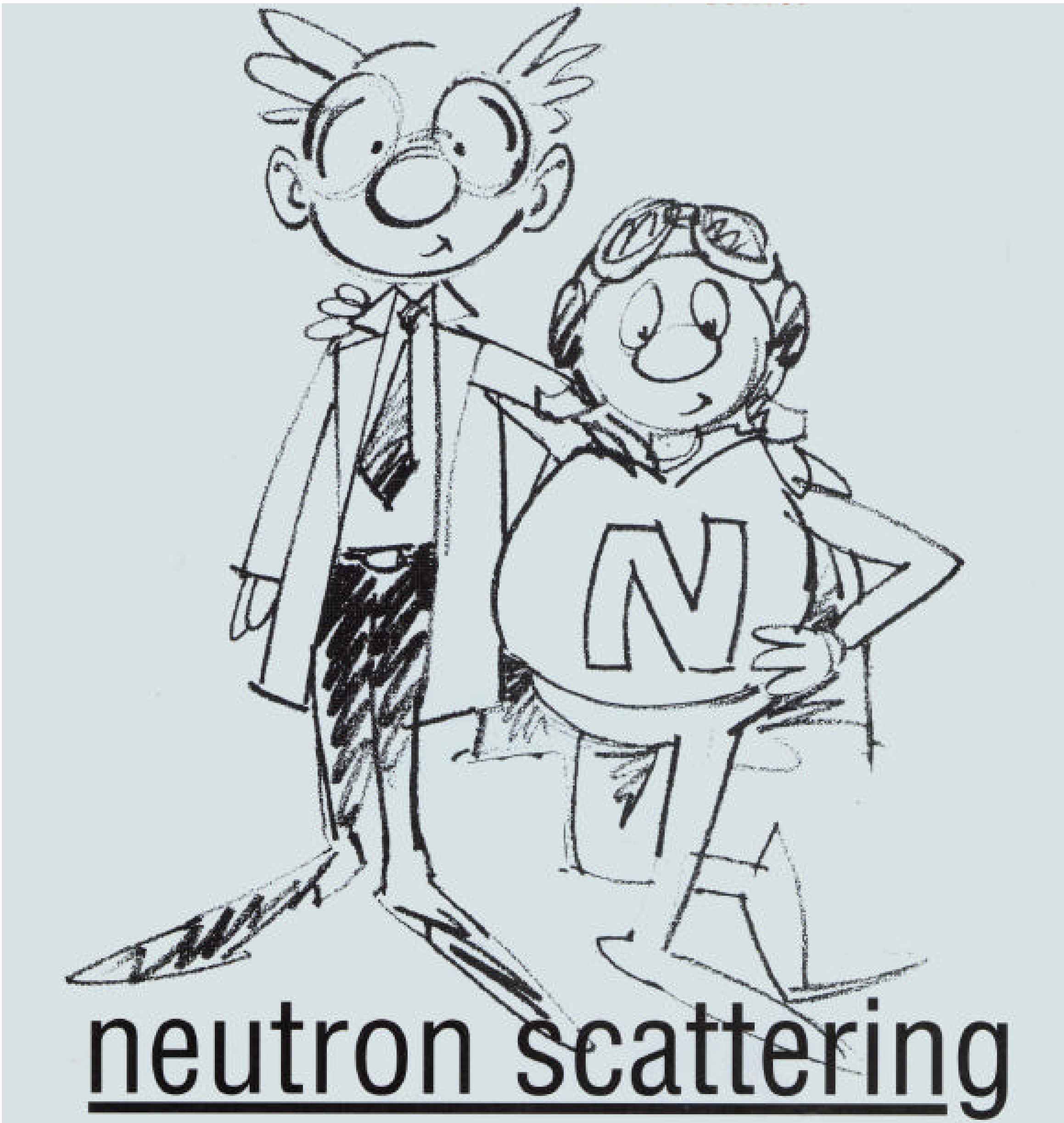

by

Roger Pynn

Los Alamos
National Laboratory

LECTURE 5: Small Angle Scattering

This Lecture

5. Small Angle Neutron Scattering (SANS)
    1. What is SANS and what does it measure?
    2. Form factors and particle correlations
    3. Guinier approximation and Porod's law
    4. Contrast and contrast variation
    5. Deuterium labelling
    6. Examples of science with SANS
        1. Particle correlations in colloidal suspensions
        2. Helium bubble size distribution in steel
        3. Verification of Gaussian statistics for a polymer chain in a melt
        4. Structure of 30S ribosome
        5. The fractal structure of sedimentary rocks

Note: The NIST web site at www.ncnr.nist.gov has several good resources for SANS – calculations of scattering length densities & form factors as well as tutorials

Small Angle Neutron Scattering (SANS) Is Used to Measure Large Objects (~1 nm to ~1 μm)

- Complex fluids, alloys, precipitates, biological assemblies, glasses, ceramics, flux lattices, long-wave-length CDWs and SDWs, critical scattering, porous media, fractal structures, etc

Scattering at small angles probes large length scales

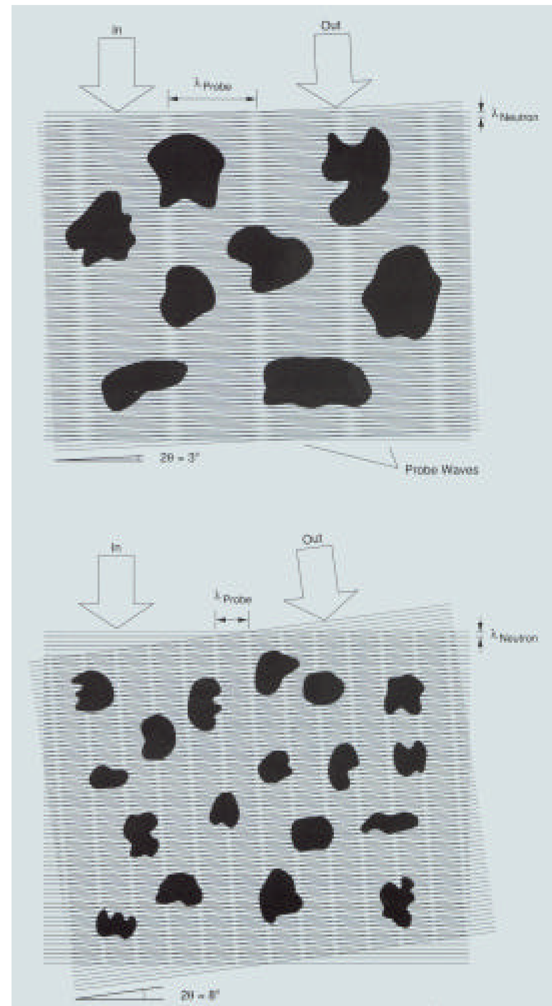

Two Views of the Components of a Typical Reactor-based SANS Diffractometer

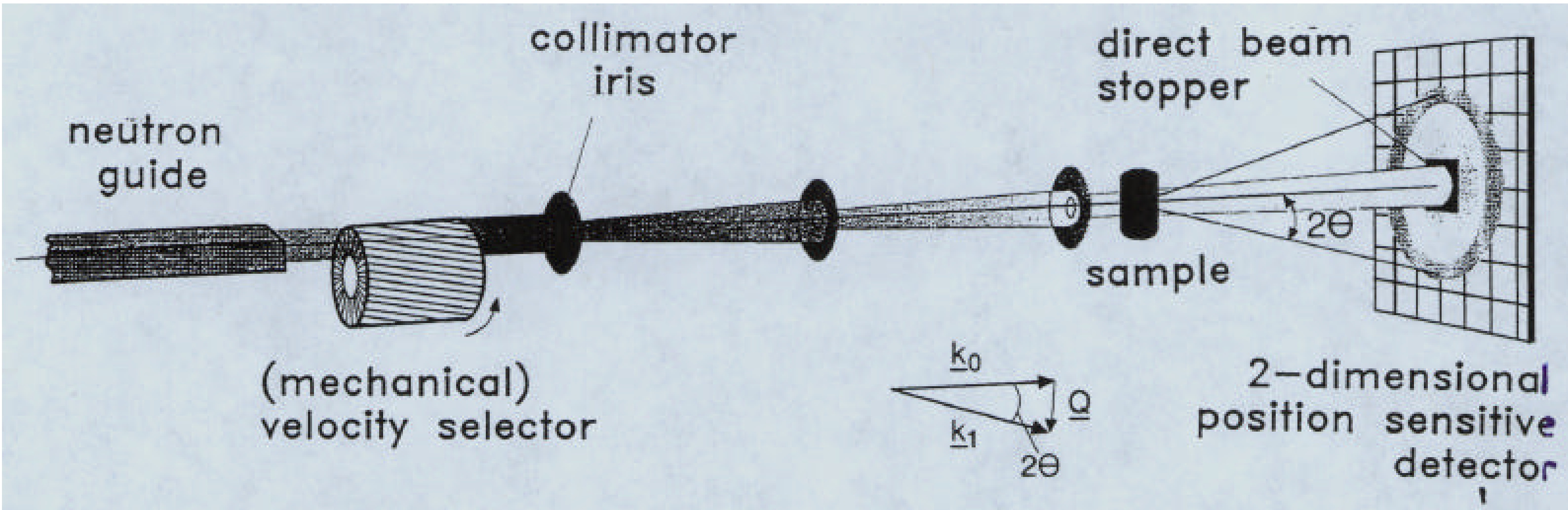

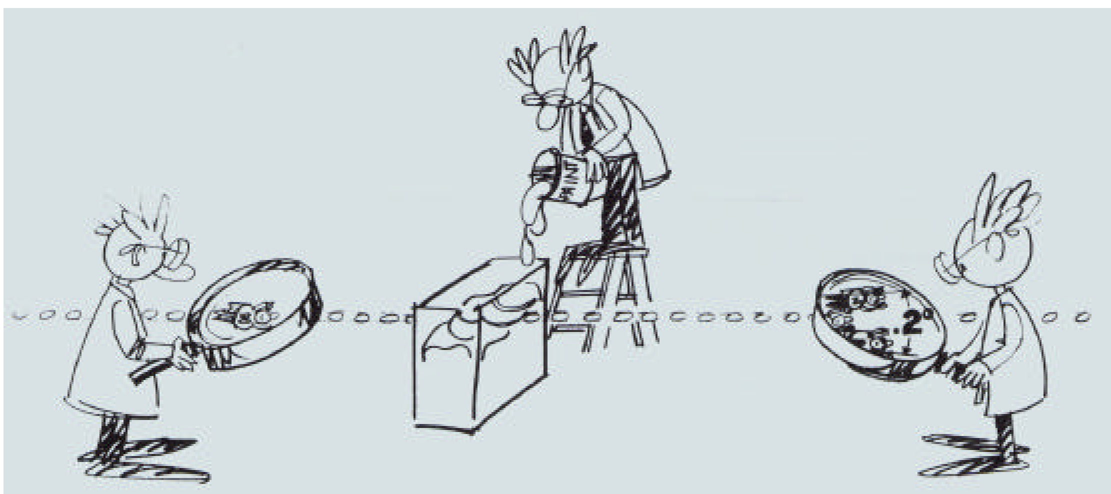

The NIST 30m SANS Instrument Under Construction

Where Does SANS Fit As a Structural Probe?

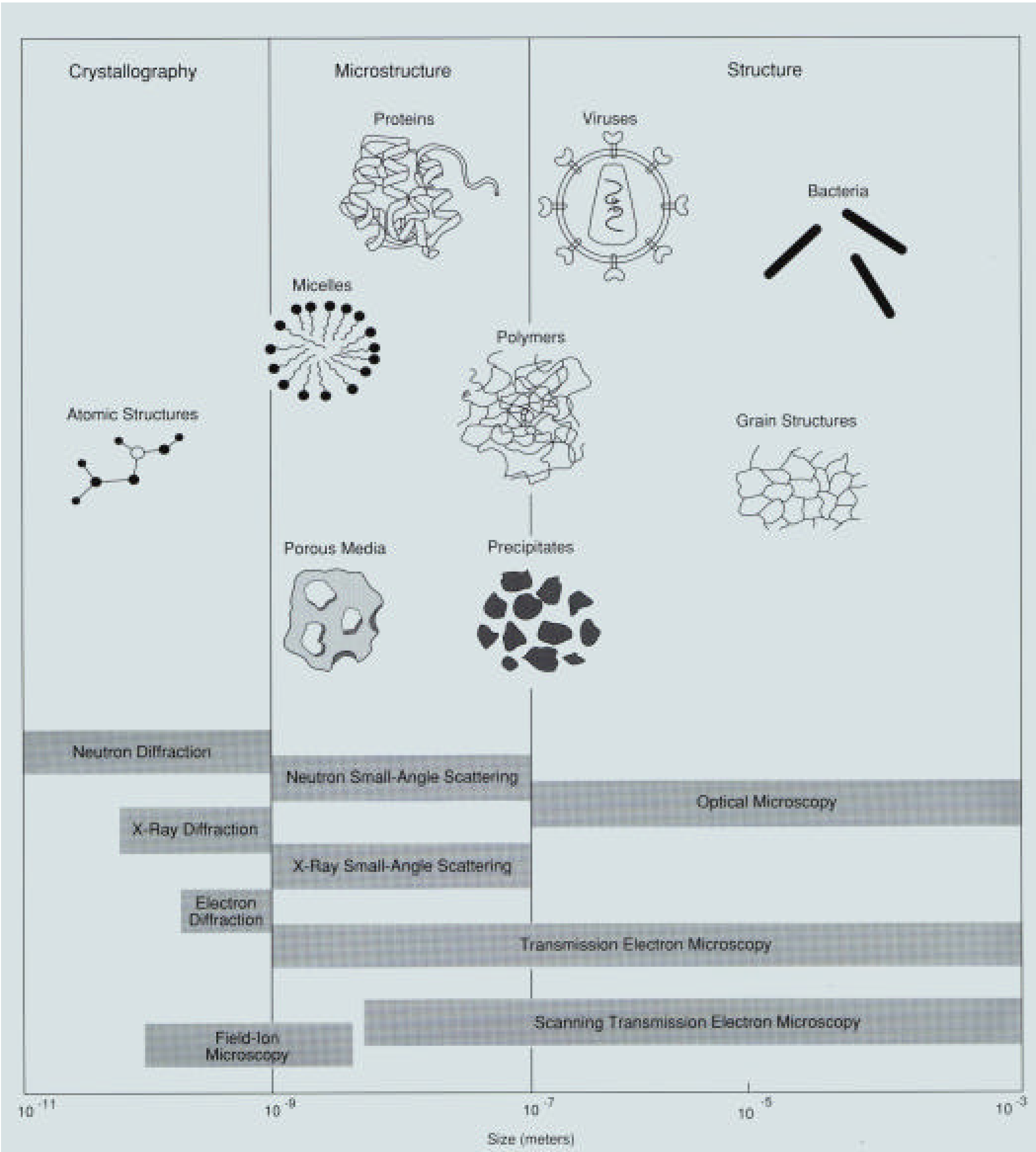

- SANS resolves structures on length scales of 1 – 1000 nm
- Neutrons can be used with bulk samples (1-2 mm thick)
- SANS is sensitive to light elements such as H, C & N
- SANS is sensitive to isotopes such as H and D

What Is the Largest Object That Can Be Measured by SANS?

- Angular divergence of the neutron beam and its lack of monochromaticity contribute to finite transverse & longitudinal coherence lengths that limit the size of an object that can be seen by SANS

- For waves emerging from slit center, path difference is hd/L if d<<h<<L; for waves from one edge of the slit path difference is (h+a)d/L

- The variation of path difference, which causes decreased visibility of Young's fringes, is ad/L so the variation in phase difference is $\Delta\psi$ = kad/L

- To maintain the visibility of the Young's interference pattern we $\Delta\psi \sim 2\pi$ so the coherence length, d ~ λ/α where α is the divergence angle a/L

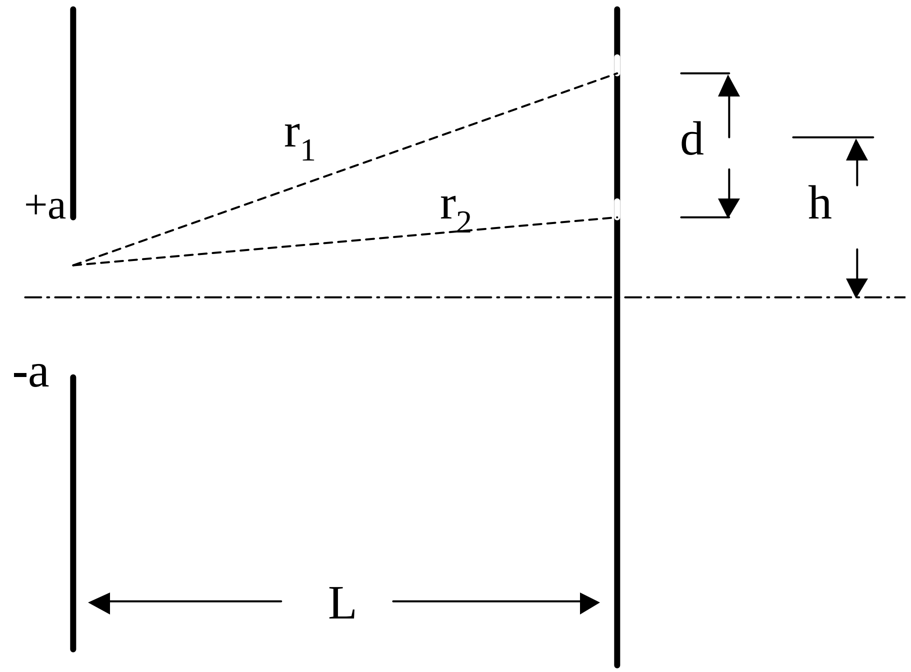

- The coherence length is the maximum distance between points in a scatterer for which interference effects will be observable

Instrumental Resolution for SANS

Traditionally, neutron scatterers tend to think in terms of Q and E resolution

$$Q = \frac{4p}{l}\sin q \;\Rightarrow\; \left\langle \frac{dQ}{Q^2}^2 \right\rangle = \left\langle \frac{dl}{l^2}^2 \right\rangle + \left\langle \frac{\cos^2 q . dq^2}{\sin^2 q} \right\rangle$$

For SANS, $(dl / l)_{rms} \sim 5\%$ and q is small, so $\left\langle \frac{dQ}{Q^2}^2 \right\rangle = 0.0025 + \left\langle \frac{dq}{q^2}^2 \right\rangle$

For equal source - sample & sample - detector distances of L and equal apertures at source and sample of h, $dq_{rms} = \sqrt{5/12}\,\mathrm{h/L}$.

The smallest value of q is determined by the direct beam size : $q_{\min} \sim 1.5 h / L$

At this value of q, angular resolution dominates and

$$d\mathrm{Q}_{\mathrm{rms}} \sim (dq_{\mathrm{rms}}/q_{\min})\mathrm{Q}_{\min} \sim dq_{\mathrm{rms}} 4p / l \sim (2p / l) h / L$$

The largest observable object is $\sim 2p/d\mathrm{Q}_{\mathrm{rms}} \sim l h / L$.

This is equal to the transverse coherence length for the neutron and achieves a maximum of about 5 mm at the ILL 40 m SANS instrument using 15 Å neutrons.

Note that at the largest values of q, set by the detector size and distance from the sample, wavelength resolution dominates.

The Scattering Cross Section for SANS

recall that $\frac{ds}{dO} = \langle b \rangle^2 NS(\vec{Q})$ where $S(\vec{Q}) = \frac{1}{N} \left\langle \left| \int d\vec{r}.e^{-i\vec{Q}.\vec{r}} n_{nuc}(\vec{r}) \right|^2 \right\rangle$

where $\langle b \rangle^2$ is the coherent nuclear scattering length and $n_{nuc}(\vec{r})$ is the nuclear density

- Since the length scale probed at small Q is >> inter-atomic spacing we may use the scattering length density (SLD), ρ, introduced for surface reflection and note that n_{nuc}(r)b is the local SLD at position **r**.

- A uniform scattering length density only gives forward scattering (Q=0), thus **SANS measures deviations from average scattering length density**.

- If ρ is the SLD of particles dispersed in a medium of SLD ρ_0, and n_p(r) is the particle number density, we can separate the integral in the definition of S(Q) into an integral over the positions of the particles and an integral over a single particle. We also measure the particle SLD relative to that of the surrounding medium I.e:

SANS Measures Particle Shapes and Inter-particle Correlations

$$\frac{ds}{d\Omega} = \langle b \rangle^2 \int_{space} d^3r \int_{space} d^3r' n_N(\vec{r}) n_N(\vec{r}').e^{i\vec{Q}.(\vec{r}-\vec{r}')}$$

$$= \int_{space} d^3R \int_{space} d^3R' \langle n_P(\vec{R}) n_P(\vec{R}') \rangle e^{i\vec{Q}.(\vec{R}-\vec{R}')} \left| (r - r_0) \int_{particle} d^3x.e^{i\vec{Q}.\vec{x}} \right|^2$$

$$\frac{ds}{d\Omega} = (r - r_0)^2 \left| F(\vec{Q}) \right|^2 N_P \int_{space} d^3R.G_P(\vec{R}).e^{i\vec{Q}.\vec{R}}$$

where G_P is the particle - particle correlation function (the probability that there is a particle at $\vec{R}$ if there's one at the origin) and $\left|F(\vec{Q})\right|^2$ is the particle form factor :

$$\left| F(\vec{Q}) \right|^2 = \left| \int_{particle} d^3x.e^{i\vec{Q}.\vec{x}} \right|^2$$

These expressions are the same as those for nuclear scattering except for the addition of a form factor that arises because the scattering is no longer from point-like particles

Scattering for Spherical Particles

The particle form factor $\left|F(\vec{Q})\right|^2 = \left|\int_V d\vec{r}\, e^{i\vec{Q}.\vec{r}}\right|^2$ is determined by the particle shape.

For a sphere of radius R, F(Q) only depends on the magnitude of Q:

$$F_{sphere}(Q) = 3V_0\left[\frac{\sin QR - QR\cos QR}{(QR)^3}\right] \equiv \frac{3V_0}{QR}\, j_1(QR) \;\rightarrow V_0 \text{ at } Q = 0$$

Thus, as $Q \rightarrow 0$, the total scattering from an assembly of uncorrelated spherical particles [i.e. when $G(\vec{r}) \rightarrow \delta(\vec{r})$] is proportional to the square of the particle volume times the number of particles.

For elliptical particles replace R by:

$R \rightarrow (a^2 \sin^2 J + b^2 \cos^2 J)^{1/2}$

where J is the angle between the major axis (a) and $\vec{Q}$

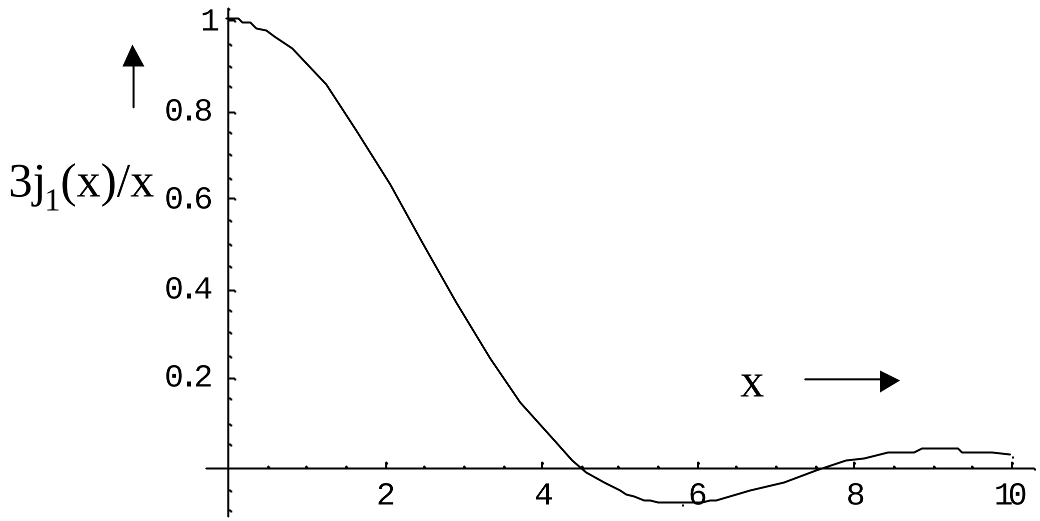

Examples of Spherically-Averaged Form Factors

Form Factor for Cylinder with Q at angle q to cylinder axis

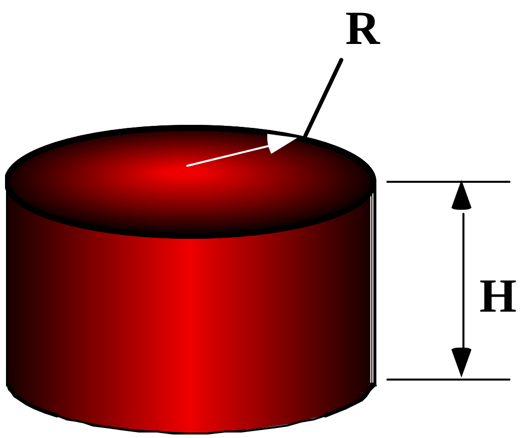

$$F(Q,q,H,R) = \frac{4V_0 \sin([QH/2]\cos q) J_1(QR \sin q)}{QH \cos q (QR \sin q)^2}$$

Form Factor for a Vesicle

$$F(Q,R,r) = 3V_0 \frac{R^2 j_1(QR) - r^2 j_1(Qr)}{Q^2(R^3 - r^3)}$$

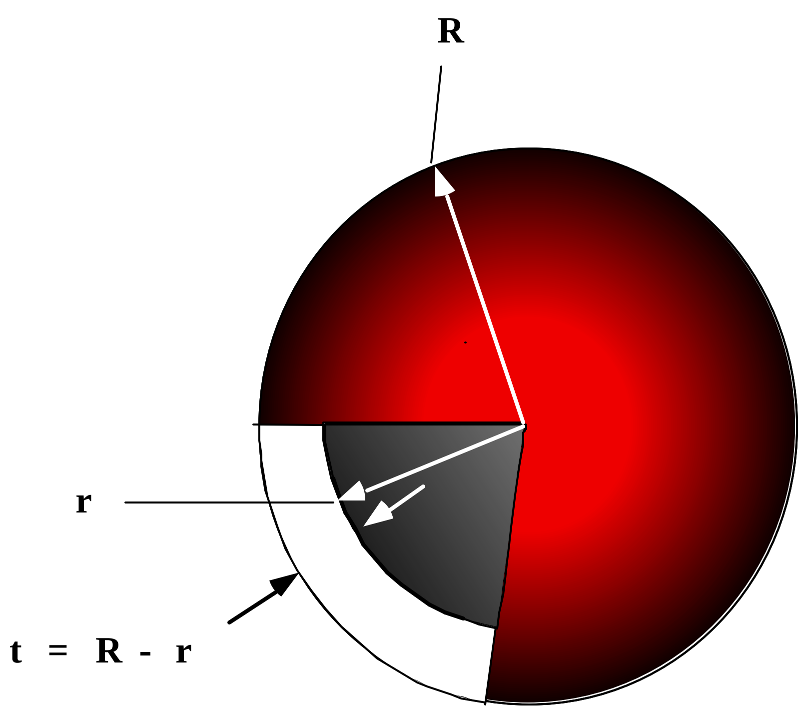

Determining Particle Size From Dilute Suspensions

- Particle size is usually deduced from dilute suspensions in which inter-particle correlations are absent
- In practice, instrumental resolution (finite beam coherence) will smear out minima in the form factor
- This effect can be accounted for if the spheres are mono-disperse
- For poly-disperse particles, maximum entropy techniques have been used successfully to obtain the distribution of particles sizes

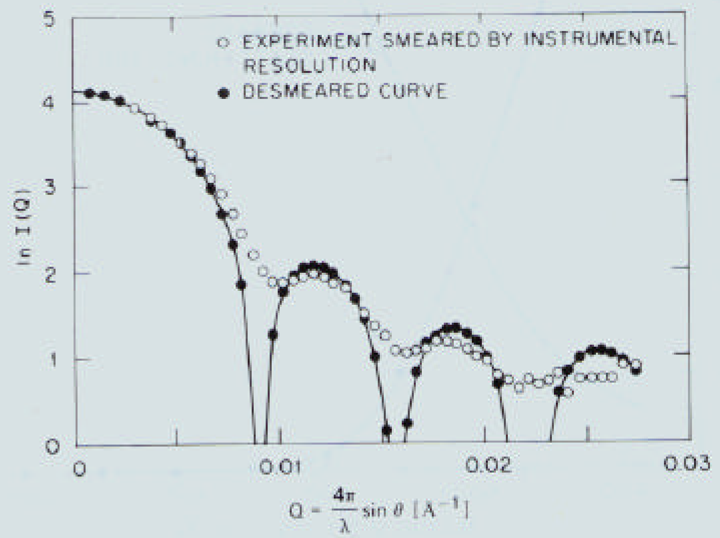

Fig. 4. Plot of ln $I(Q)$ *vs* Q for 3·98 vol.% monodisperse PMMA-H spheres (core $C1$) in D_2O/H_2O mixtures.

Correlations Can Be Measured in Concentrated Systems

- A series of experiments in the late 1980's by Hayter et al and Chen et al produced accurate measurements of S(Q) for colloidal and micellar systems
- To a large extent these data could be fit by S(Q) calculated from the mean spherical model using a Yukawa potential to yield surface charge and screening length

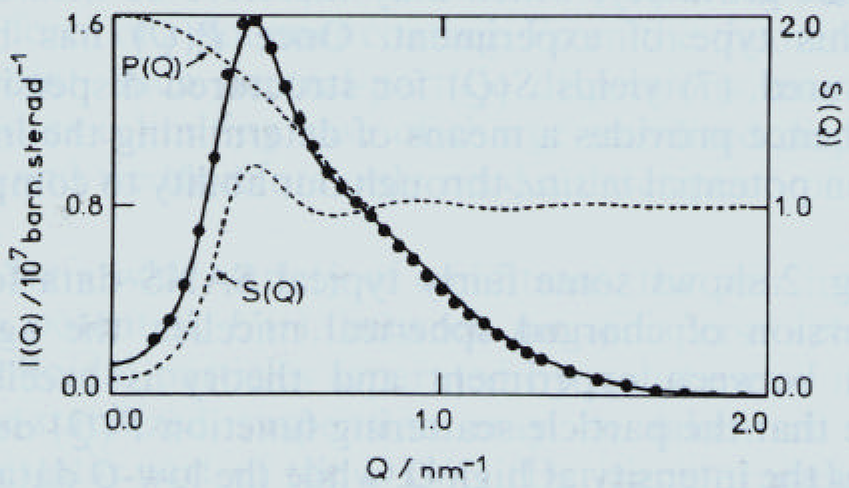

Fig. 2. Observed (●) and calculated (——) scattered intensity $I(Q)$ as a function of momentum transfer Q for a charged micellar dispersion: 0·03 mol dm^{-3} hexadecyltrimethylammonium chloride in D_2O at 313 K. The functions $P(Q)$ and $S(Q)$ are discussed in the text. (1 barn sterad^{-1} = 10^{-28} M^2 sterad^{-1}).

Size Distributions Have Been Measured for Helium Bubbles in Steel

- The growth of He bubbles under neutron irradiation is a key factor limiting the lifetime of steel for fusion reactor walls
  - Simulate by bombarding steel with alpha particles
- TEM is difficult to use because bubble are small
- SANS shows that larger bubbles grow as the steel is annealed, as a result of coalescence of small bubbles and incorporation of individual He atoms

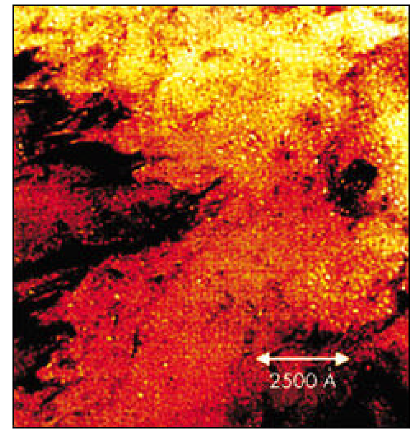

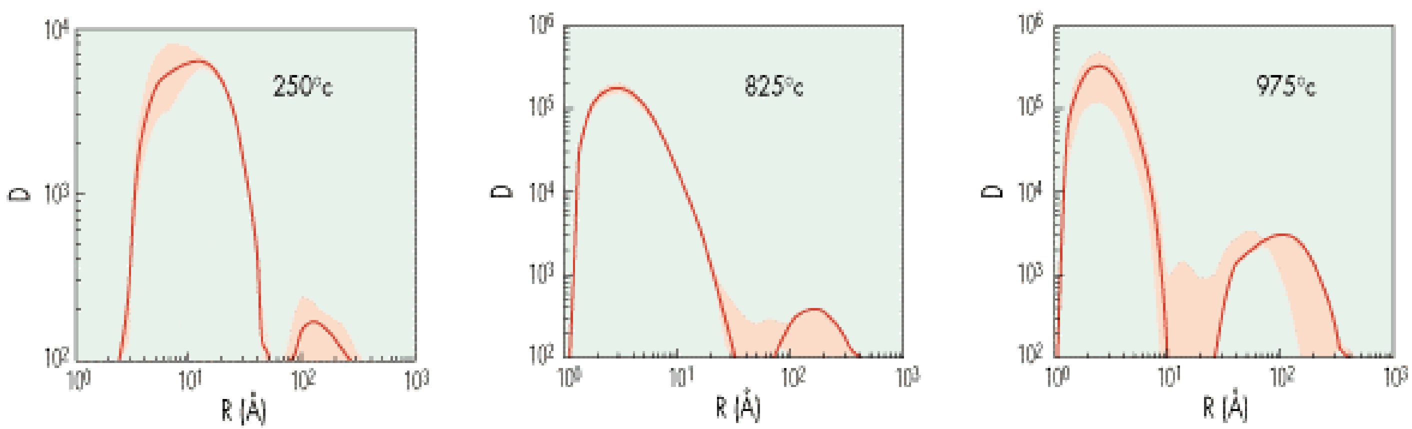

SANS gives bubble volume (arbitrary units on the plots) as a function of bubble size at different temperatures. Red shading is 80% confidence interval.

Radius of Gyration Is the Particle "Size" Usually Deduced From SANS Measurements

If we measure $\vec{r}$ from the centroid of the particle and expand the exponential in the definition of the form factor at small Q:

$$F(Q) = \int_V d\vec{r} e^{i\vec{Q}.\vec{r}} \approx V_0 + \cancel{i\int_V \vec{Q}.\vec{r} d^3 r} - \frac{1}{2}\int_V (\vec{Q}.\vec{r})^2 d^3 r + ...$$

$$= V_0 \left[1 - \frac{Q^2}{2} \frac{\int_0^p \cos^2 q \sin q . dq}{\int_0^p \sin q . dq} \frac{\int_V r^2 d^3 r}{\int_V d^3 r} + ... \right] = V_0 \left[1 - \frac{Q^2 r_g^2}{6} + ... \right] \approx V_0 e^{-\frac{Q^2 r_g^2}{6}}$$

where r_g is the radius of gyration is $r_g = \int_V R^2 d^3 r / \int_V d^3 r$. It is usually obtained from a fit to SANS data at low Q (in the so-called Guinier region) or by plotting ln(Intensity) v Q^2. The slope of the data at the lowest values of Q is $r_g^2/3$. It is easily verified that the expression for the form factor of a sphere is a special case of this general result.

Guinier Approximations: Analysis Road Map

Generalized Guinier approximation

$$\langle P(Q)\rangle = \begin{Bmatrix} 1; & \alpha = 0 \\ \alpha\pi Q^{-\alpha}; & \alpha = 1,2 \end{Bmatrix} \Delta M_{\alpha 0} \exp\left(-\frac{R_\alpha^2 Q^2}{3-\alpha}\right)$$

Derivative-log analysis

$$\frac{d \ln\langle P(Q)\rangle}{d \ln(Q)} = \frac{Q}{\langle P(Q)\rangle}\frac{d\langle P(Q)\rangle}{dQ} = -\alpha - \frac{2}{3-\alpha}R_\alpha^2 Q^2$$

Guinier Law

$$\lim_{Q \to 0} I(Q) = \Delta M_0 \exp\left(-\frac{R_g^2 Q^2}{3}\right)$$

$$\Delta M_0 = V^2\left(\bar{\rho}_p - \rho_s\right)^2$$

$$R_g = \frac{1}{V}\int \rho(r) r^2 dv_r$$

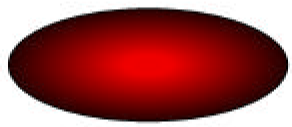

Guinier Law for a rod

$$I(Q) = \frac{\pi}{Q}\Delta m_0 \exp\left(-\frac{R_c^2 Q^2}{2}\right)$$

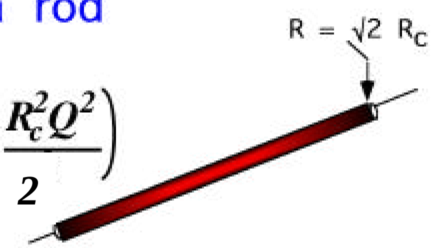

Guinier Law for a sheet

$$I(Q) = \frac{2\pi}{Q^2}\Delta\mu_0 \exp\left(-R_d^2 Q^2\right)$$

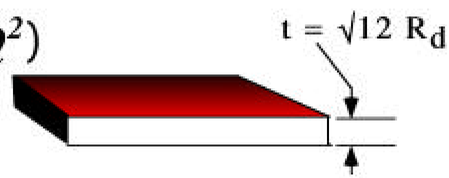

- Guinier approximations provide a roadmap for analysis.
- Information on particle composition, shape and size.
- Generalization allows for analysis of complex mixtures, allowing identification of domains where each approximation applies.

* Viewgraph courtesy of Rex Hjelm

Contrast & Contrast Matching

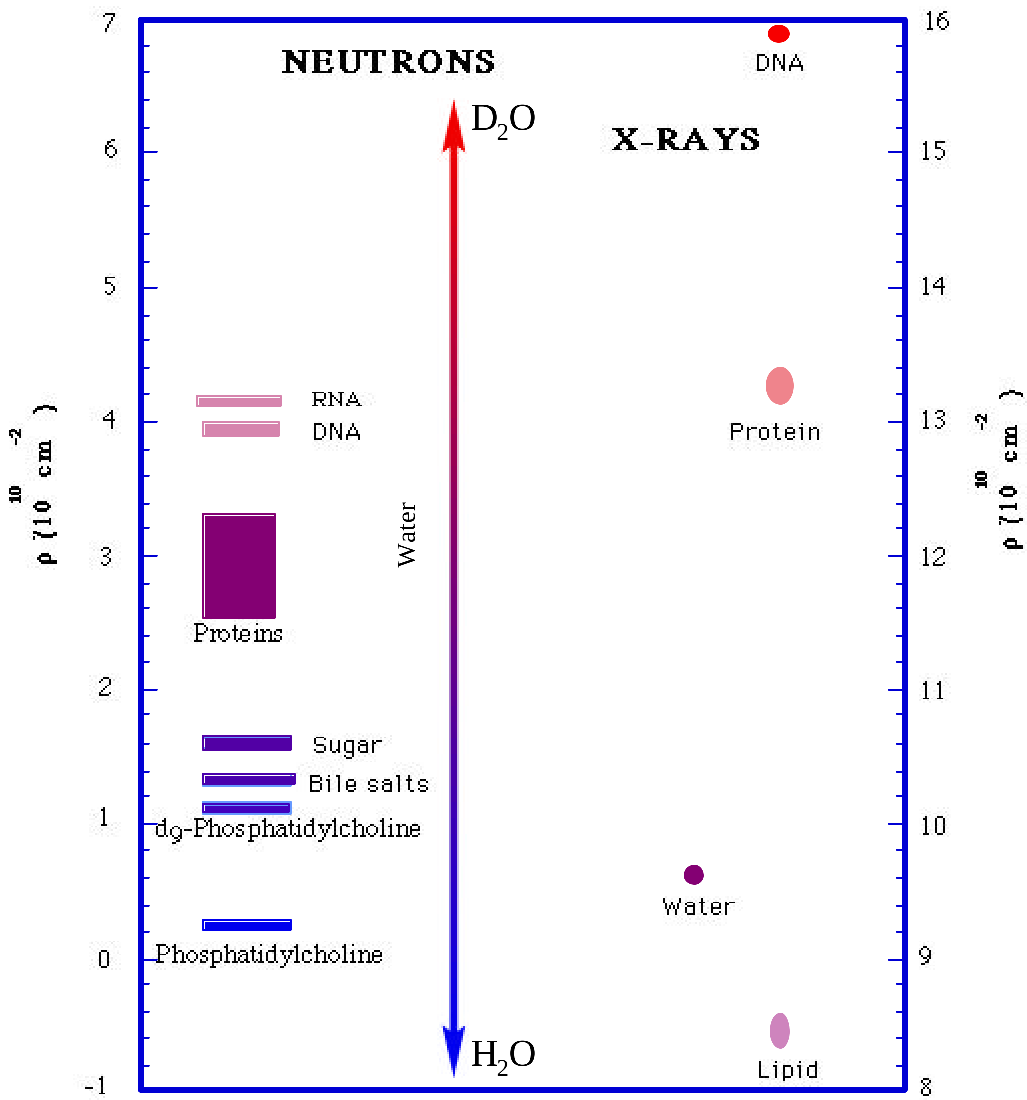

* Chart courtesy of Rex Hjelm

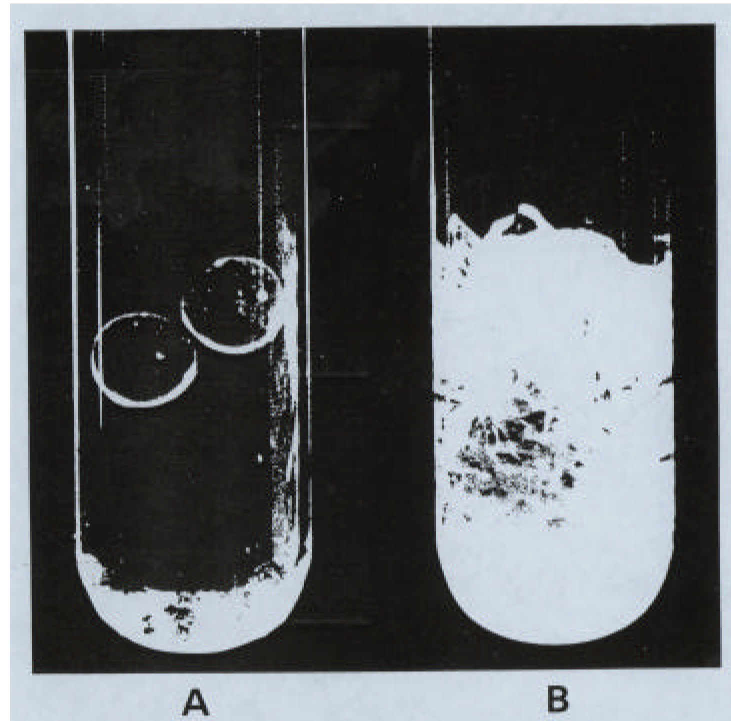

Both tubes contain borosilicate beads + pyrex fibers + solvent. (A) solvent refractive index matched to pyrex;. (B) solvent index different from both beads and fibers – scattering from fibers dominates

Isotopic Contrast for Neutrons

Hydrogen Isotope	Scattering Length b (fm)
^{1}H	-3.7409 (11)
^{2}D	6.674 (6)
^{3}T	4.792 (27)

Nickel Isotope	Scattering Lengths b (fm)
^{58}Ni	15.0 (5)
^{60}Ni	2.8 (1)
^{61}Ni	7.60 (6)
^{62}Ni	-8.7 (2)
^{64}Ni	-0.38 (7)

Verification of of the Gaussian Coil Model for a Polymer Melt

- One of the earliest important results obtained by SANS was the verification of that $r_g \sim N^{-1/2}$ for polymer chains in a melt

- A better experiment was done 3 years later using a small amount of H-PMMA in D-PMMA (to avoid the large incoherent background) covering a MW range of 4 decades

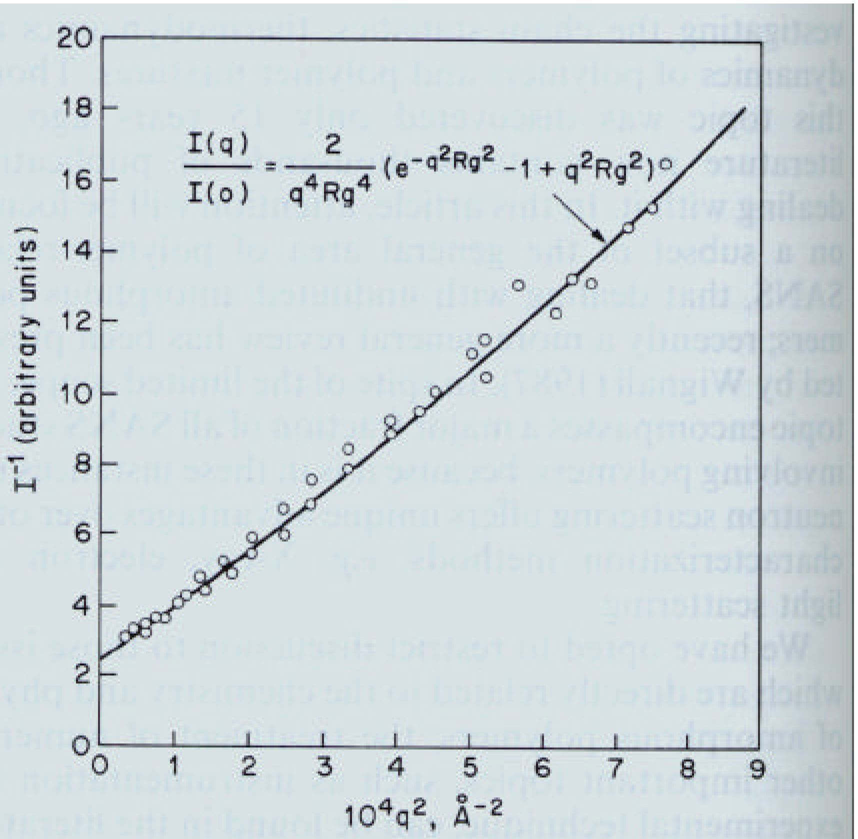

Fig. 1. SANS results obtained by Kirste, Kruse & Schelten (1972) for 1·2% deuterated poly(methyl methacrylate) (PMMA) in normal PMMA (mol. wt of 250 000) plotted in Ornstein–Zernike form. The solid curve represents a Debye function [equation (1)]. This was one of the first quantitative demonstrations of Gaussian coil behavior for bulk polymers.

SANS Has Been Used to Study Bio-machines

- Capel and Moore (1988) used the fact that prokaryotes can grow when H is replaced by D to produce reconstituted ribosomes with various pairs of proteins (but not rRNA) deuterated
- They made 105 measurements of inter-protein distances involving 93 30S protein pairs over a 12 year period. They also measured radii of gyration
- Measurement of inter-protein distances is done by Fourier transforming the form factor to obtain G(R)
- They used these data to solve the ribosomal structure, resolving ambiguities by comparison with electron microscopy

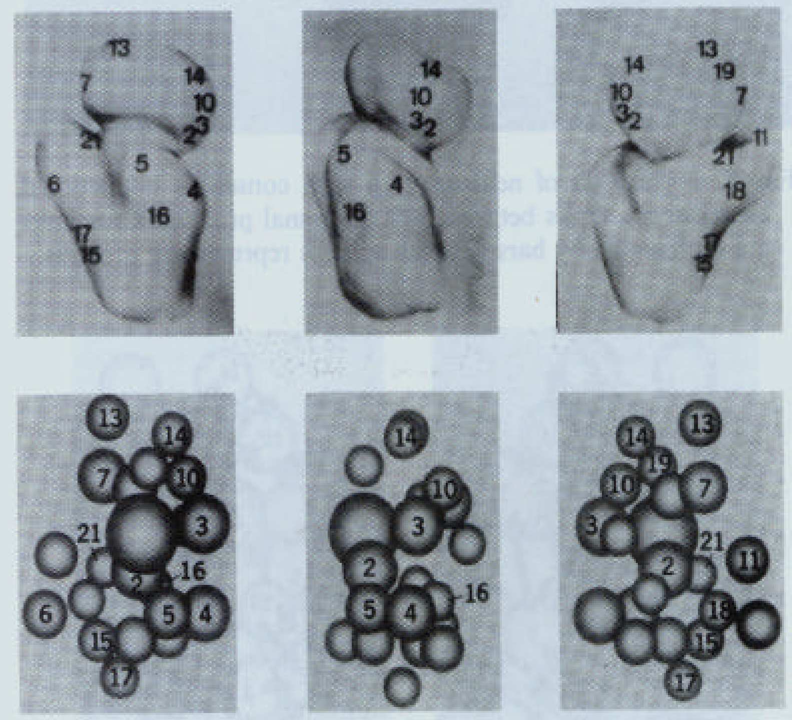

Fig. 4. Comparison of neutron map with a mapping of surface-exposed antigenic sites of ribosomal proteins of the 30S subunit obtained by immune-electron microscopy (Stoeffler & Stoeffler-Meilicke, 1986).

Porod Scattering

Let us examine the behavior of $|F(Q)|^2 (QR)^4$ at large values of Q for a spherical particle (i.e. Q >> 1/R where R is the sphere radius)

$$|F(Q)|^2 (QR)^4 = 9V^2 \left[\frac{\sin QR - QR.\cos QR}{(QR)^3}\right]^2 (QR)^4 = 9V^2 \left[\frac{\sin QR}{QR} - \cos QR\right]^2$$

$$\rightarrow 9V^2 \cos^2 QR \text{ as } Q \rightarrow \infty$$

$$= 9V^2/2 \text{ on average (the oscillations will be smeared out by resolution)}$$

Thus $|F(Q)|^2 \rightarrow \frac{9V^2}{2(QR)^4} = \frac{2pA}{Q^4}$ where A is the area of the sphere's surface.

This is Porod's law and holds as $Q \rightarrow \infty$ for any particle shape provided the particle surface is smooth.

Another way to obtain it is to expand $G(r) = 1 - ar + br^2 + ..$[with $a = A/(2pV)$] at small r and to evaluate the form factor with this (Debye) form for the correlation function.

Scattering From Fractal Systems

- Fractals are systems that are "self-similar" under a change of scale I.e. R -> CR
- For a mass fractal the number of particles within a sphere of radius R is proportional to R^D where D is the fractal dimension

Thus

$$4pR^2 dR.G(R) = \text{number of particles between distance R and R} + \text{dR} = cR^{D-1}dR$$

$$\therefore\ G(R) = (c/4p)R^{D-3}$$

$$\text{and}\ \ S(\vec{Q}) = \int d\vec{R}.e^{i\vec{Q}.\vec{R}}G(R) = \frac{2p}{Q}\int dR.R.\sin QR.(c/4p)R^{D-3}$$

$$= \frac{c}{2}\frac{1}{Q^D}\int dx.x^{D-2}.\sin x = \frac{const}{Q^D}$$

For a surface fractal, one can prove that $S(Q) \propto \dfrac{const}{Q^{6-D_s}}$ which reduces to the Porod form for smooth surfaces of dimension 2.

Typical Intensity Plot for SANS From Disordered Systems

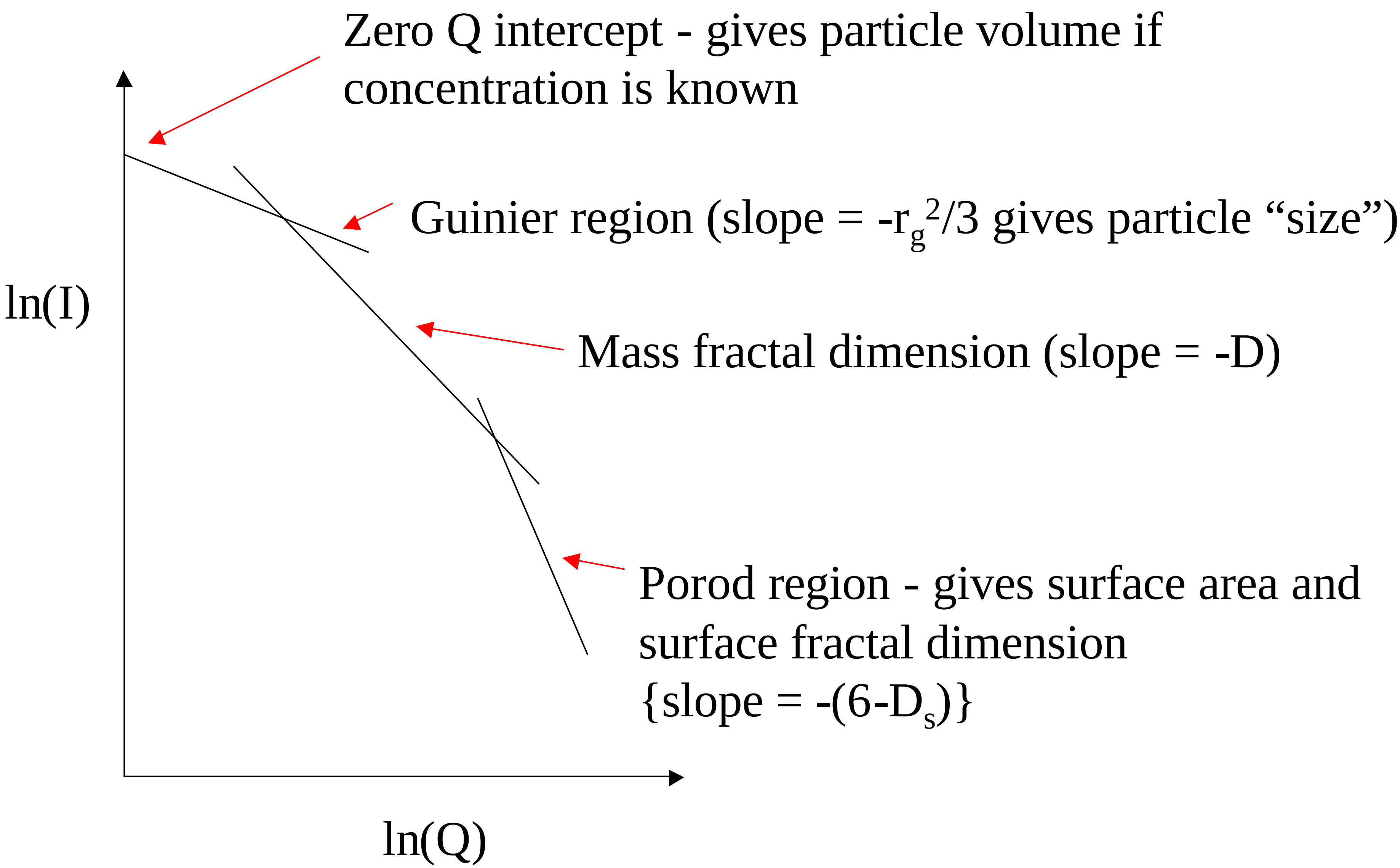

Sedimentary Rocks Are One of the Most Extensive Fractal Systems*

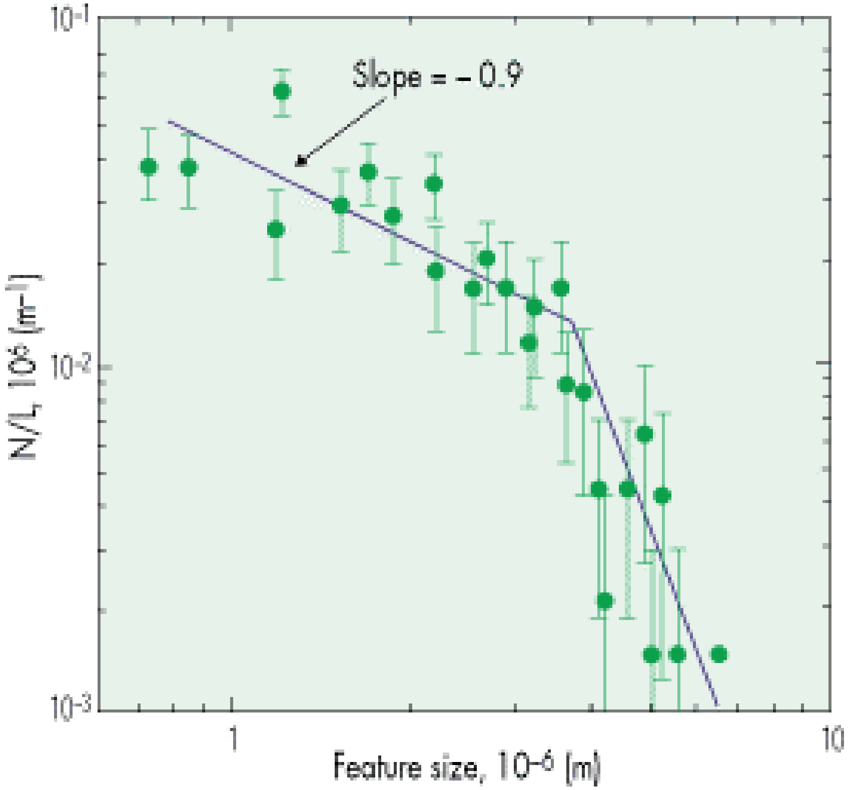

Variation of the average number of SEM features per unit length with feature size. Note the breakdown of fractality (D_s=2.8 to 2.9) for lengths larger than 4 microns

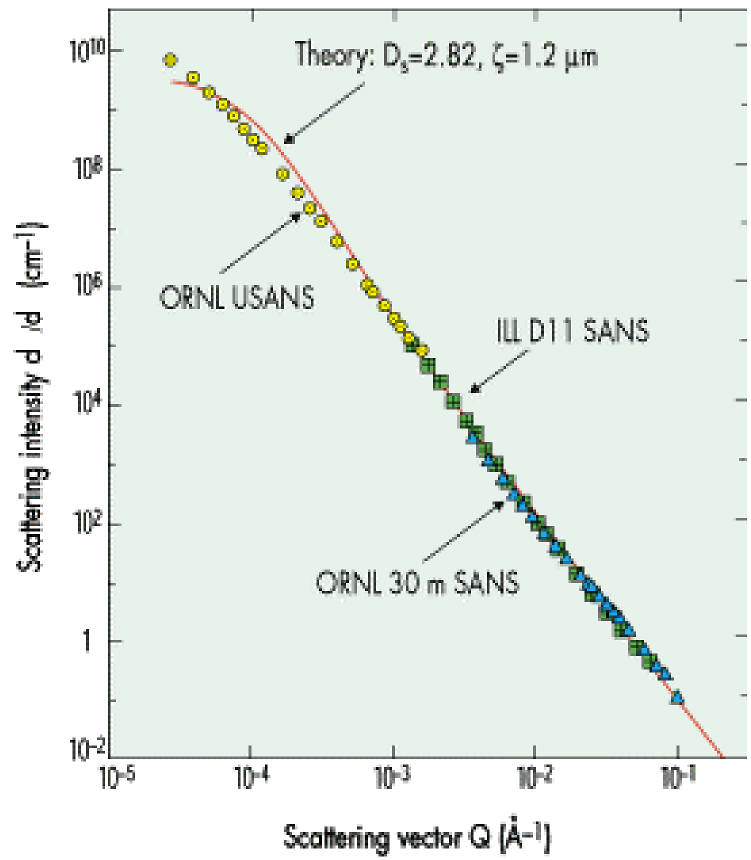

SANS & USANS data from sedimentary rock showing that the pore-rock interface is a surface fractal (D_s=2.82) over 3 orders of magnitude in length scale

*A. P. Radlinski (Austr. Geo. Survey)

References

- Viewgraphs describing the NIST 30-m SANS instrument
  - http://www.ncnr.nist.gov/programs/sans/tutorials/30mSANS_desc.pdf